Retaining soil wall treated with cement: centrifuge modelling

M. Castaneda-Lopez[1], T. Lenoir[1*], J.-P. Sanfratello[2], P. Hauza[3], T. Dubreucq[4], L. Thorel[4], P. Audrain[4], A. Neel[4], A. Jagu[4], S. Lerat[4], P. Gaudicheau[4]

[1]*University Gustave Eiffel, Advanced Materials for Transportation Infrastructures Laboratory, F-44344 Bouguenais, France*
[2]*Independent expert, 78340 Les Clayes-sous-Bois, France,*
[3]*Technical, Research and Development Management, COLAS compagny, 78771 Magny-les-Hameaux, France*
[4]*University of Gustave Eiffel, Centrifuge for Geotechnic Laboratory, F-44344 Bouguenais, France*
* *Corresponding author: thomas.lenoir@univ-eiffel.fr*

ABSTRACT: Cement stabilization is a common technique used to enhance the engineering and mechanical properties of in-situ soils in accordance with the stress rates imposed by civil engineering projects. Using in-situ soils with hydraulic binders reduces reliance on quarried materials, minimizing environmental impact and infrastructure costs. Cement-stabilized soils (CSS) have many applications in civil engineering, mainly embankments, pavements, and railway construction. This study aims to evaluate CSS as a construction material for retaining walls. First, laboratory-scale studies were conducted to characterize the elastic and shear strength properties of a CSS. Then, a centrifuge study was conducted on a scale-down cement-stabilized retaining wall (CSRW). A scaled CSRW model was built and tested under 20×g centrifuge acceleration to simulate 4 m wall height with no surcharge. Centrifuge test results are very encouraging for the large-scale use of CSRW.

1 INTRODUCTION

In cement-stabilized retaining walls (CSRW) the strength of the soil mass is improved by the addition of cement without any reinforcing strip, bar or geosynthetic. In principle, CSRW should be designed as a conventional mass-structure and the stability of the wall may be investigated following conventional limit equilibrium method. The first documented reference about cement-stabilized retaining walls is the study done by Morris and Crockford (Morris, 1993; Morris & Crockford, 1991). They report the design, construction and monitoring of real scale CSRW (two walls, 4.9 and 7.0 m heights) part of an overpass structure in Houston, Texas (US). At experimental scale, mechanical performances of the treated soil was assessed by means of triaxial tests and unconfined compressive strength (UCS). Similar methodology, based on UCS, was employed by Chandler and Palmer (1999) for a part of an overpass structure of a locality near Sydney, Australia. The wall described in their study is the largest CSRW documented with a high varying between 8 m and 22 m and a length of 450 m. Numerical modeling was done using fast lagrangian analysis of continua. Ismail (2005) present a more general study of a CSRW based on numerical and physical modeling. The plane-strain finite element analysis was carried out using the PLAXIS code. Both, the retained and the treated soil were modeled as $c - \varphi$ materials.

In order to study, among other things, the impact of the compaction by elementary layers of such a wall on shear strength, Gustave Eiffel University and the COLAS company established a research agreement to determine whether cement-stabilized soils (CSS) could be used as construction material for retaining structures.

From a mechanical point of view, this issue was addressed at three different observation scales. First, at the laboratory scale, on test specimens, in order to characterize the mechanical performance and mechanical constitutive laws of the CSS. At the real-scale (Figure 1.a), a 4 m high CSRW (Figure 1.b). was constructed and instrumented in the Nantes Campus of the University Gustave Eiffel. At a reduced scale, several reduced CSRW models were built and tested under centrifuge acceleration.

At all, five 1/20th scaled CSRW models were built and tested under centrifugal accelerations ranging from 20×g to 60×g to simulate wall heights from 4 to 12 meters. The backfill was loaded with a surcharge equal to typical road loading. Through these tests, we have determined the influence of the bearing soil's deformability on the CSRW. Secondly, we have examined the structure's ability to withstand critical conditions induced by model saturation, including the degradation of CSS properties and increased active thrust from the backfill. Finally, we sought to determine whether variability in CSS preparation significantly impacts the structure's performance by reducing the quantities of cement, the compaction rate, and the curing time.

The present article reports the study of the reduced scale CSRW model at 20×g for one of the CSSs, without surcharge, in order to reproduce the real scale construction of the CSRW . Others cited studies will be reported in future articles.

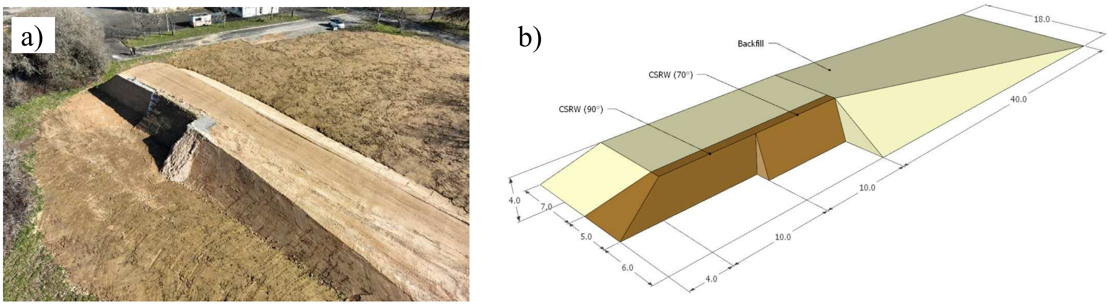

Figure 1. a) Real scale CSRW in Nantes Campus; b) Dimensions (meters) of CSRW (brown) and backfill (yellow), dimensions in meters

2 EXPERIMENTAL DESIGN

2.1 Experimental programm

The physical model reduced to 1/20th scale consists of (Figure 2.a): the CSRW, the sandy backfill, which is retained by the CSRW, the sandy foundation beneath which supports both the wall and the backfill.

The model is placed in a container with a transparent face to allow an image analysis of the structure during the flight thanks to an on-board camera and a lighting (Figure 2.b). The container is 80 cm long and 30 cm wide. A thin polyvinyl chloride angle is placed on the slope behind the wall to prevent the passage of sand between the wall edge and the front glass. The model is subjected to centrifuge acceleration $N_g \times g = 20 \times 9.81$ m/s² applied to the base of the wall. The scale model is designed according to the scaling laws of physical modelling (Table 1, Garnier et al., 2001).

Table 1. Wall dimensions

Parameters	**Prototype**	**Model**
height H (mm)	4000	200
base B (mm)	5000	250
Wall top b (mm)	1000	50
Length L (mm)	6000	300

During centrifuging, the stresses in the model are identical to those in the prototype in order to reproduce identical internal frictions (cohesion, friction angle) within the sandy backfill, ground foundation, and the CSRW.

2.2 Instrumentation

Image analysis to evaluate displacements or shear strains was conducted using GeoPIV-RG software (Stanier et al., 2016). In parallel, Picture software (Moliard, 1993) was used to monitor the trajectories of visual markers located behind the container window (Figure 2.a). In the tested setup (Figure 2.b), the image analysis camera (acA4112-8gm/gc, Basler©) provides a resolution better than 0.1 mm at model scale.

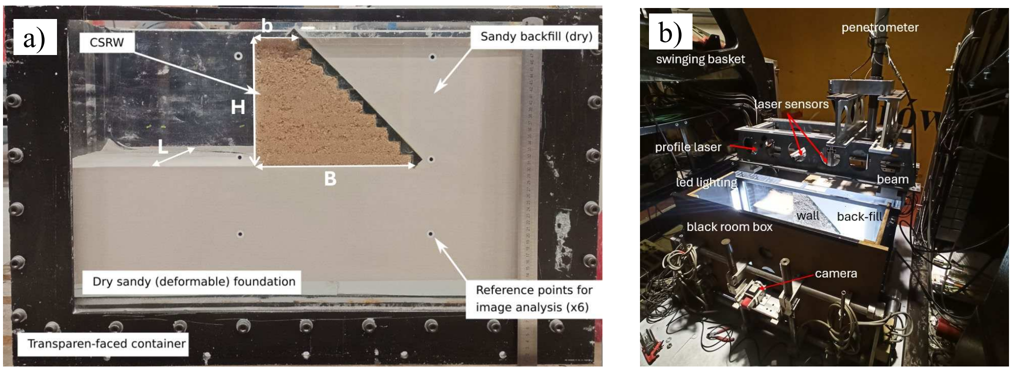

Figure 2. a) Reduced scale CSRW model in transparent-faced container; b) the model installed in the centrifuge basket

Vertical displacements of reference points (D) of the wall top and of the backfill are monitored using respectively laser sensors Wenglor© (resolution 20µm) Baumer© (resolution 20µm) (Figure 3a). Total pressure (P) is monitored with two sensors beneath the wall along the central axis (Figure 3.b).

A vertical laser profile Baumer© (resolution 20µm) is continuously recorded to capture displacement variations along the façade of the CSRW. These sensors have an accuracy of ±0.1 mm.

In-flight soil characterization was undertaken using a miniature cone penetrometer test. CPT tests were undertaken using a 1-D actuator with a displacement rate of 2 mm/s. The average diameter of the cone penetrometer is 12 mm.

2.3 Material

2.3.1 Soil for retaining wall

The geo-material is a quarry tailing from Chauvé, France. The maximum diameter of larger elements in this material is less than 50 mm. Through an 8 mm sieve, the cumulated undersize is 93%, and fine content, less than 80 µm, is 17%, which means that its mechanical behavior was controlled by its coarse fraction. It is classified as coarse-grained soil (AFNOR, 2018d). Despite a high clay activity, A = PI/$C_{2\mu m}$ = 1.3, the low clay content and low PI imply a low swelling potential. The results of characterization are resumed in Table 2 and the grain size curve is shown in Figure 4.

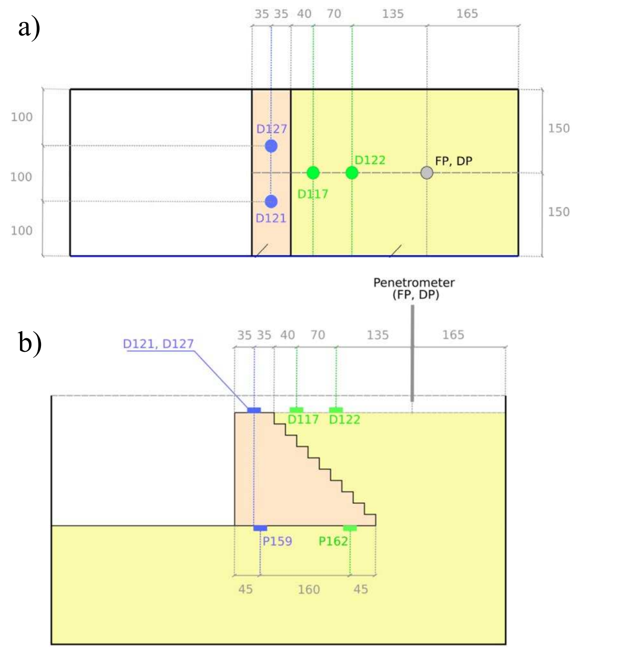

Figure 3. Sensors locations; a) plan view; b) in section. CSS in brown and NE34 sand in yellow. Unit: mm in model scale)

2.3.2 Treated soil in retaining wall

For the cement ctabilized coil (CSS), the variables used to describe a given mixture are curing time (CT) in days, cement content (CC) as percentage of dry material weight and degree of compaction (DC) as percentage of MDD. Soil was treated with CC = 3% (weight of dry material) of CEM II/A-LL 42.5 R, a Portland-limestone composite cement (composition:clinker (K, 80-94%), limestone (A-LL, 6 to 20 %) and minor additional constituents (0-5%)). The class of strength is 42.5 R, a high early strength cement, with a compressive strength higher than 20 MPa at 2 days, and between 42.5 and 62.5 MPa at 28 days (AFNOR, 2012).

Table 2. Physical properties of soil

Properties	**Soil**
clay content (d < 2 µm)[a], $C_{2\mu m}$	6%
silt (2 µm < d < 63 µm)[a]	11%
sand (63 µm < d < 2 mm)[a]	40%
gravel (2 mm < d < 200 mm)[a]	43%
AASHTO[b] classification	A-2-6(0)
GTR[c] classification	B6
USCS[d] classification	SM-SC

[a]Soil size range based on European standard NF EN ISO 14688-1 (AFNOR, 2018a); [b] American Association of State Highway and Transportation Officials; [c] French Road Earthworks Manual; [d] Unified Soils Classification System.

Lime pre-treatment was not needed due to the suitable workability. The Optimum Moisture Content (OMC) and Maximum Dry Density (MDD) relationships were obtained following Proctor compaction tests (AFNOR, 2014) for standard compaction effort. OMC = 10.0% and MDD = 1.98 g/cm^3. Treated mixture is prepared at 96% of MDD and at the OMC.

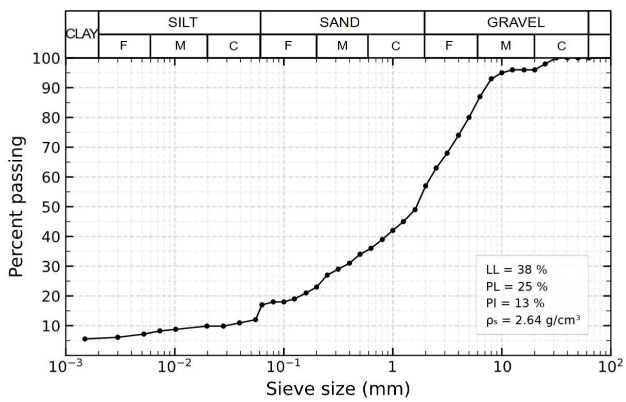

Figure 4. Particle-size distribution of the studied soils

For this reference mixture, mechanical properties were measured at several CT (Table 4).

The strength properties of the reference mixture were measured at the laboratory scale. These were quantified using the following features and standards: unconfined compressive strength (UCS), according to NF EN 13286-41 (AFNOR, 2021); indirect tensile strength (ITS), according to NF EN 13286-42 (AFNOR, 2003a) and direct shear strength according to NF EN ISO 17892-10 (AFNOR, 2018b).

For the direct shear test, five levels of normal stress varying from 2 to 250 kPa were used, and the Mohr-Coulomb criterion was used to represent the shear strength of the treated material, namely the c_{app} apparent cohesion, and ϕ_{app} apparent friction angle. The measured properties are presented in Table 3. All properties were measured under unsaturated conditions (water content equal to OMC).

Table 3. Mohr-Coulomb properties of CSS.

CT (days)	UCS (MPa)	ITS (MPa)	Mohr-Coulomb		
			c_{app} (MPa)	ϕ_{app} (°)	R^2
7	0.91 (0.03)	0.12 (0.01)	0.178	49.4	0.98
28	1.20 (0.03)	0.17 (0.01)	0.266	53.0	0.94
90	1.53 (0.18)	0.21 (0.01)	0.382	49.5	0.93
180	1.72 (0.07)	0.26 (0.01)	0.385	42.4	0.82
360	1.91 (0.04)	0.31 (0.01)	0.406	61.3	0.86

Standard deviation (SD) in brackets.

The elastic properties of the reference mixture were determined during UCS test measurements. Local displacements were measured using Hall-effect transducers. The procedure for determining the elastic modulus E_{CCS} and Poisson's ratio ν_{CCS} was slightly adapted from the standard EN 13286-43:2003 (AFNOR, 2003b). Based on the shapes of displacement curves, an appropriated interval, within which the slopes of the axial stress-axial strain and radial strain-axial strain curves were quantified. The measured elastic properties are summarized in Table 4.

The complete experimental dataset and details of experimental set-up, measuring devices and procedures is available in public repositorie (Castaneda-Lopez et al., 2023 and 2025).

Table 4. Elastic properties of CSS using UCS tests

CT (days)	E_{CCS} (MPa)	ν_{CCS} (-)
7	1459 (42)	0.15 (0.03)
28	1281 (206)	0.10 (0.05)
90	1672 (151)	0.15 (0.04)
180	969 (12)	0.17 (0.05)
360	1271 (182)	0.14 (0.05)

Standard deviation (SD) in brackets

2.3.3 Fontainebleau sand

The soil fondation consists of a medium-dense Fontainebleau sand (Nemours, France) NE34 (mean grain size d_{50}= 0.21 mm; coefficient of uniformity C_u= 1.47; coefficient of curvature C_c= 1.05, Dano et al., 2024). NE34 is implemented by rainfall owing to a hopper whose height and speed of translation are controlled at each pass (about 5 mm layer thickness) to ensure a homogeneous density and a density index of I_d = 0.73 of soil foundation. Its density measured with box at the bottom is 1680 kg/m^3 for a friction angle equal to 40° and a zero cohesion (direct shear tests, NF EN ISO 17892-10). Then the CRSW is deposited in the container. Its presence during rainfall involves the appearance of a layer slope (figure 5), which reduced the fall height in the close vicinity of the back wall, and therefore leading to a reduction in sand density. A thin seal is placed against the glass to prevent sand from falling into glass-wall interface.

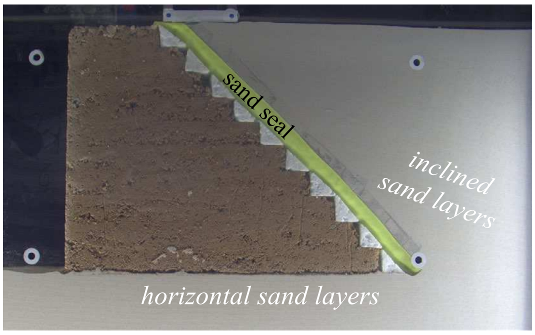

Figure 5. Effect of wall presence during sand rainfall

2.4 Compaction of the CSRW

CSS is compacted in static mode at the OMC and compaction degree DC = 96% to obtain the density $\rho_{d\ CSWR}$ = 1.90 g/cm^3, in a steel mold (Figure 6.a), with CC=3 %.

This steel mold serves to contain the CSRW during preparation, while interchangeable auxiliary aluminum plates, screw-fixed to the mobile plate, are used to create the stepped profile (Figure 6.b).

The volume of the CSRW model is 9600 mm^3 which for the aimed DC corresponds to a weight of 20.1 kg. Ten layers with the same individual thickness of 20 mm conform the CSRW (Figure 6.c). Compaction time respect the workability time of the treated soil.

Widths of auxiliary plates and auxiliary pistons vary by layer, requiring the arrangement to be readjusted before each compaction stage. Auxiliary plates are fixed to the mobile plate to limit the risk of developing failure surfaces within the CSS during compaction.

DC = 96.2 % is checked at CT = 35 days of curing time, just before centrifuge test. Table 5 summarizes the associated mechanical characteristics of CCS taken from measurements after CT = 28 days (E_{CCS}, $\phi_{app\ (35\ days)}$) and by interpolation (c_{app}).

Table 5. Elastic and Mohr-Coulomb properties of CSS

$E_{CCS\ (35\ days)}$ (MPa)	$c_{app\ (35\ days)}$ (MPa)	$\phi_{app\ (35\ days)}$ (°)
1281	0.328	53

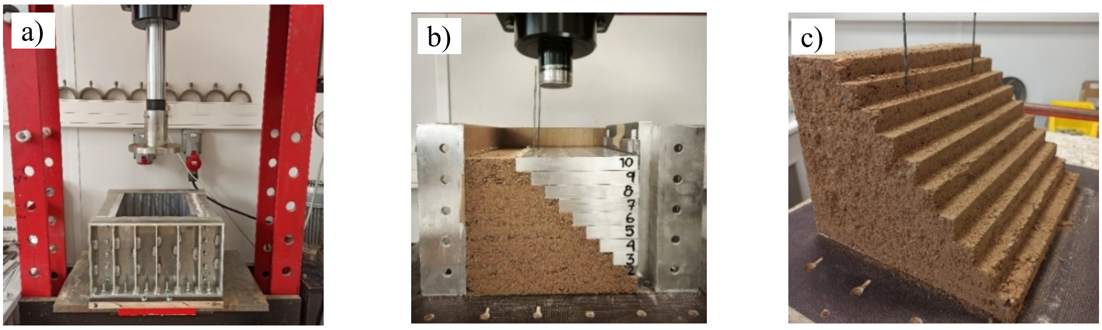

Figure 6. a) Compacting of the CSS in a rigid mould; b) 10-layer compacted wall; c) unmolded wall

3 RESULTS AND ANALYSIS

3.1 Rise from 1 to 20×g in centrifuge

The centrifuge acceleration from 1 to 20×g progressively, called "g-rise" thereafter, increases in order to move from the reduced model dimension to the prototype dimensions. It is thus increased in stages: 5×g, 10×g, 15×g and finally 20×g. Each level lasts 5 minutes.

It then goes back down to 1×g. The sequence is reapeted twice, in order to stabilize the displacements in the model. At the end of the last 3rd g-rise, the creep level begins, at 20×g for 1 hour about (Figure 7.a).

Total pressure measurements are generally very tricky because they highky dependent of the placement of the sensors and contact quality (Figure 7.b). The vertical total stress (P162 ≈ 170 kPa) at the 3rd g-rise under the wall at its back remains positive at 20×g.

The stress under the wall at the front (P159 ≈ 94 kPa) is about two times lower. The average stress (≈ 132 kPa) is twice as high as that of calculated from the weight of the wall and the sand wedge above (≈ (0.6×1900+0.4×1680)×9.81×4 = 71 kPa). This result can be explained by a probable concentration of vertical forces on these two rigid sensors.

Qualitatively, settlements of the wall and of the backfill stabilize quickly with the g-rises (Figures 7.c and 7.d). The part of the wall towards the rear of the container goes down, while the part towards the glass side seems not settling.

To be precise, the values should be corrected with the very little bending deflection of the strong beams that support the laser sensors, during g-rises.

Then, during the 1 hour creep phase at 20×g, the displacements are negligible. Only the vertical stress under the wall at the back decreases by a few kilopascals.

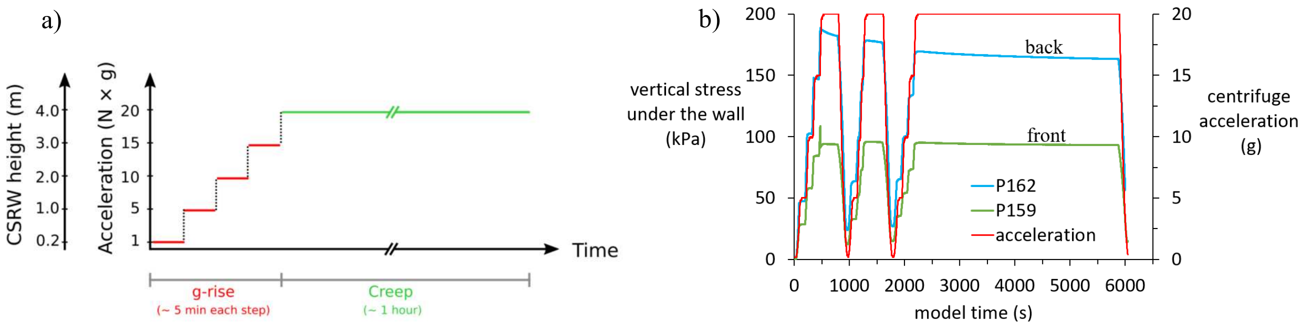

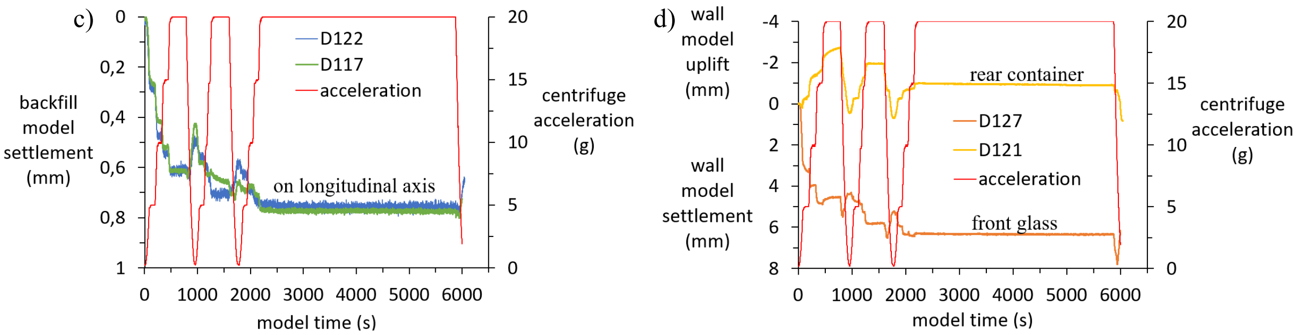

Figure 7: a) Evolution of acceleration (exemple of the 3rd g-rise) ; b) vertical total stress under the wall; c) backfill settlement ; d) wall settlement

3.2 Image analysis

3.2.1 Wall, backfill and foundation displacements

During the g-rise, the fixation of the camera and the beam device become deformed, which requires first the introduction of corrections while moving, especially in the vertical plane.

This correction is made possible thanks to the six markers fixed to the inner glass of the non-deformable container (Figure 8). The apparent displacements of each marker are then determined by image analysis with "Picture" software, between the 1×g image and the 20×g image. Thus we deduce an average correction. It is then applied to the displacements of the wall, the backfill and the ground foundation, after image analysis with "GeopIV" (Figures 9 and 10).

The trapezoidal wall and its back sand wedge above it move together horizontally forward by about 0.15 mm in figure 8 (0.15×20 = 3 mm in prototype size). This displacement is close to H/1000 by lower value, and corresponds to the mobilization of the limit horizontal pressure of the embankment behind this sand wedge. The sandy foundation moves horizontally and slightly in front and behind the wall, to a depth of about B/2.

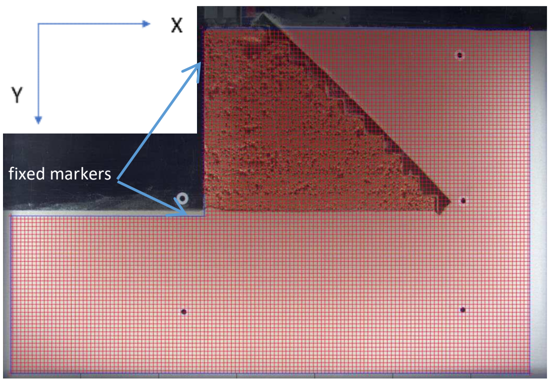

Figure 8. Image analysis for g-rise; tracking the movements of the 6 fixed markers between the 1×g image and the 20×g image; square mesh in red (25×25 pixels)

The settlement of the wall is 0.6 mm in figure 9 (0.6×20= 12 mm in prototype). Beneath, the settlement of sandy foundation is about 0.2 mm and 0.5 mm, at the back and front of the wall respectively (4 mm and 10 mm in prototype). It reveals a small rotation of the wall. The average settlement is far from the threshold of 3%×B corresponding to the permissible settlement.

The vertical displacements in the sand wedge attached to the wall are of the order of 0.8 mm in figure 9 (0.8×20 = 16 mm in prototype). This value is comparable to the surface settlement measured by the D117 and D122 laser sensors.

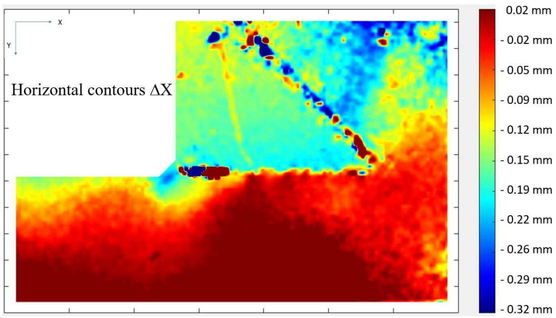

Figure 9. Horizontal displacement in model scale, for wall, sandy foundation and sandy backfill (after 3rd g-rise).

We can also see the Coulomb wedge at the back of the wall (sliding line inclined at $\pi/4+\phi_{sand}/2 = 65°$ from the horizontal), with internal vertical displacements of the order of 0.4 mm (0.4×20= 8 mm in prototype).

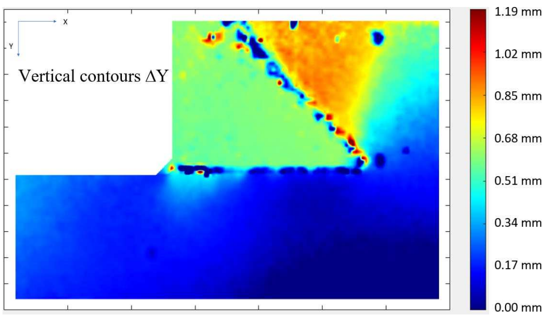

Figure 10. Settlement in model scale in CSRW, sandy foundation and backfill, from 1×g to 20×g (after 3rd rise).

3.3 Front wall displacement profile

The displacement profile of the wall is also measured with a laser positioned in front of the wall (Figure 11).

The average horizontal displacement is about 0.2 mm (0.2×20 = 4 mm in prototype). No failure deformation, such as a slippage between compacted layers, is detectable at 20×g. This value is comparable to that measured by image analysis previously.

The overall displacement of the wall, the backfill, and the sandy foundation indicates that this CSRW is behaving normally in service. Subsequently, this same model of CRSW was centrifuged to 60×*g* to simulate a 12 m high prototype: similarly, no internal failure was still observed (study not reported here).

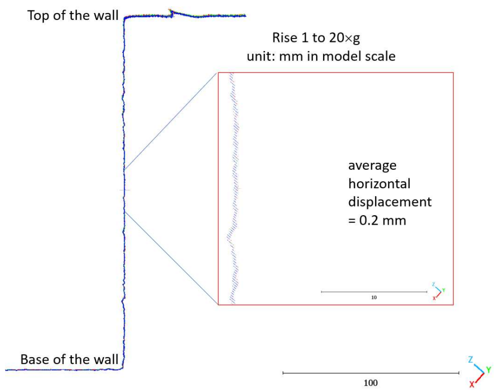

Figure 11. Displacement of the front wall (3rd g-rise).

3.4 Foundation bearing capacity

To be able to determine the bearing capacity of foundation beneath the wall, a penetrometer test was carried out at the end of the creep, in the close vicinity of the back wall (Figure 12). Average slopes for backfill and foundation are ~ 23 mm/MPa and ~ 11 mm/MPa, respectively, in relation with the higher density of sand placed beneath the wall compared to the density just behind it (see §.2.3.3).

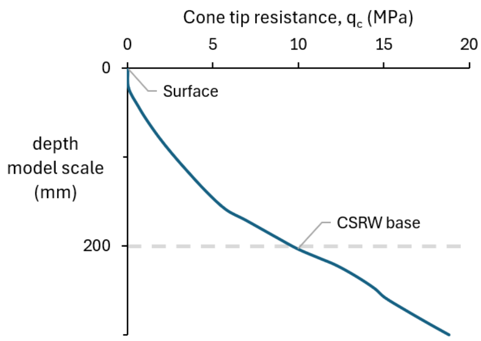

Figure 12. Cone tip resistance as a function of penetration depth in model scale.

4 CONCLUSIONS

The first results of centrifuge tests were presented for a 1/20th scale model wall in soil lightly treated with cement (3% in mass) and compacted in elementary layers at 96% of MDD and at the OMC, to simulate a real scale wall built on the Nantes Campus of the University Gustave Eiffel.

The prototype wall was trapezoidal in shape, 4 m high, 5 m wide at the base, with a 1 m wide platform at the top with no surcharge. It was made with a silty sand treated with 3% of cement by dry mass, then compacted into 10 layers of 40 cm thick each.

After 35 days of curing time, the 1/20th scale model wall presented a cohesion value of 0.328 MPa and a friction angle of 53°. It was placed in a transparent-faced container above a sandy foundation, and withstood a sandy embankment. Centrifuged at 20×g, displacement measurements do not showed any internal fracture of the cement-stabilized retaining wall. The settlement and horizontal displacement in the model revealed a normal behavior for a gravity wall under service conditions.

In particular, no slippage between the compacted layers was observed. In practice, a quick compaction of the real wall is needed over its entire height while respecting the workability time.

The remaining tests (surcharge at top of the wall; saturation of wall, backfill and ground foundation; degradation of CC and DC) are currently under analysis. Preliminary results suggets that a less robust geometry, with a reduced wall witdth at the base, could also be considered.

ABBREVIATIONS

CSRW : cement-stabilized retaining walls
CSS : cement-stabilized soils

NOTATIONS

B : width of the wall base [mm]
b : width of the wall top [mm]
L : length of the wall [mm]
H : height of the wall [mm]
c_{app} : apparent cohesion of CSRW [MPa]
ϕ_{app} : apparent friction angle of CSRW [°]
ϕ'_{sand} : Fontainebleau sand friction angle [°]
CC : cement content (dry weight percentage) [%]
C_c : coefficient of curvature [-]
CT : curing time [days]
C_u : coefficient of uniformity [-]
$C_{2\mu m}$: clay content [%]
DC : compaction degree as MDD percentage [%]
D_r : relative density [%]

d_{50} : mean grain size [mm]
E_{CCS} : elastic modulus of CSS [MPa]
g : earth acceleration : 9.81 m/s² [-]
I_d : sand density index [-]
ITS : indirect tensile strength [MPa]
N_g : number of g applied to the model [-]
MDD : maximum dry density [g/cm^3]
OMC : optimum moisture content [%]
PI : plasticity index [%]
q_c : cone tip resistance [MPa]
S_r : degree of saturation [%]
UCS : unconfined compressive strength [MPa]
ν_{CCS} : Poisson's ratio of CCS [-]
$\rho_{d\ \mathrm{sand}}$: dry density of sand[kg/m^3]
ρ_{CRSW} : density of CSRW [kg/m^3]
Δx / Δy : horizontal / vertical displacement [mm]

REFERENCES

AASHTO. (2021). *M 145-91. Classification of Soils and Soil–Aggregate Mixtures for Highway Construction Purposes*.

AFNOR. (2003a). *NF EN 13286-42. Unbound and hydraulically bound mixtures - Part 42 : test method for the determination of the indirect tensile strength of hydraulically bound mixtures*.

AFNOR. (2003b). *NF EN 13286-43. Unbound and hydraulically bound mixtures Part 43: Test method for the determination of the modulus of elasticity of hydraulically bound mixtures*.

AFNOR. (2012). *NF EN 197-1. Cement - Part 1: Composition, specifications and conformity criteria for common cements*.

AFNOR. (2014). *NF P94-093. Soils : Investigation and testing — Determination of the compaction reference values of a soil type — Standard Proctor Test — Modified Proctor Test*.

AFNOR. (2018a). *NF EN ISO 14688-1. Geotechnical investigation and testing - Identification and classification of soil - Part 1 : identification and description*.

AFNOR. (2018b). *NF EN ISO 17892-10. Geotechnical investigation and testing - Laboratory testing of soil - Part 10 : direct shear tests*.

AFNOR. (2018d). *NF EN ISO 17892-4. Geotechnical investigation and testing - Laboratory testing of soil - Part 4 : Determination of particle size distribution*.

AFNOR. (2021). *NF EN 13286-41. Unbound and hydraulically bound mixtures - Part 41: test method for the determination of the compressive strength of hydraulically bound mixtures*. AFNOR.

Castaneda-Lopez, M. A., Lenoir, T., Thorel, L., Sanfratello, J. P. (2023). Tensile properties of cement stabilized soils: experimental data. https://doi.org/10.57745/DFW5LS

Castaneda-Lopez, M. A., Lenoir, T., Thorel, L., Sanfratello, J. P. (2025). Unconfined Compressive Strength and Mohr–Coulomb properties of cement stabilized soils: experimental data. https://doi.org/10.57745/L6EIIT

Castaneda-Lopez, M., Lenoir, T., Sanfratello, J.-P., & Thorel, L. (2023). Data-Driven Prediction of Cement-Stabilized Soils Tensile Properties. *Infrastructures*, *8*(10), 146. https://doi.org/10.3390/infrastructures8100146

Castaneda-Lopez, M., Lenoir, T., Thorel, L., Sanfratello, J.-P. (2025). Determination of Mohr–Coulomb Failure Criterion of Cement-Treated Materials Using Mixture Design Properties. *Infrastructures*, *10*(10), 267. https://doi.org/10.3390/infrastructures10100267

Chandler, K. R., & Palmer, M. (1999). Design and Construction of a Cement Stabilised Sandstone Retaining Wall. Proceedings 8th Australia New Zealand Conference on Geomechanics, 739–746. https://search.informit.org/doi/10.3316/informit.737753270744675

Dano, C., Thorel, L., Dupla, J.-C., Benahmed, N., & Li, Z. (2024). Compilation des propriétés physiques et mécaniques du sable de Fontainebleau NE34. *Revue Française de Géotechnique*, *c*(179), 6. https://doi.org/10.1051/geotech/2024027

Garnier, J., Gaudin, C., Springman, S. M., Culligan, P. J., Goodings, D., Konig, D., Kutter, B., Phillips, R., Randolph, M. F., & Thorel, L. (2007). Catalogue of scaling laws and similitude questions in geotechnical centrifuge modelling. *International Journal of Physical Modelling in Geotechnics*, *7*(3), 01–23. https://doi.org/10.1680/ijpmg.2007.070301

Ismail, M. A. (2005). Performance of cement-stabilized retaining walls. Canadian Geotechnical Journal, 42(3), 876–891. https://doi.org/10.1139/t05-021

Moliard J M. (1993) Logiciel Picture: Outil de traitement d'images appliqué aux essais en centrifugeuse. *Rapport LCPC*; 54p.

Morris, D. V. (1993). Monitoring of cement stabilized soil retaining walls. 80.

Morris, D. V, & Crockford, W. W. (1991). Design of cement stabilized soil retaining walls with concrete panel facing. In Texas Transportation Institute.

Stanier S, Blaber J, Take W, White D. (2016) Improved image-based deformation measurement for geotechnical applications. *Can. Geotech. J.*; 53 (5), 727-739. https://doi.org/10.1139/cgj-2015-0253.